JB
Journals.ASM.org

Two DHH Subfamily 1 Proteins in *Streptococcus pneumoniae* Possess Cyclic Di-AMP Phosphodiesterase Activity and Affect Bacterial Growth and Virulence

Yinlan Bai,[a]* Jun Yang,[a] Leslie E. Eisele,[b] Adam J. Underwood,[a] Benjamin J. Koestler,[c] Christopher M. Waters,[c] Dennis W. Metzger,[a] Guangchun Bai[a]

Center for Immunology and Microbial Disease, Albany Medical College, Albany, New York, USA[a]; Wadsworth Center, New York State Department of Health, Albany, New York, USA[b]; Department of Microbiology and Molecular Genetics, Michigan State University, East Lansing, Michigan, USA[c]

Cyclic di-AMP (c-di-AMP) and cyclic di-GMP (c-di-GMP) are signaling molecules that play important roles in bacterial biology and pathogenesis. However, these nucleotides have not been explored in *Streptococcus pneumoniae*, an important bacterial pathogen. In this study, we characterized the c-di-AMP-associated genes of *S. pneumoniae*. The results showed that SPD_1392 (DacA) is a diadenylate cyclase that converts ATP to c-di-AMP. Both SPD_2032 (Pde1) and SPD_1153 (Pde2), which belong to the DHH subfamily 1 proteins, displayed c-di-AMP phosphodiesterase activity. Pde1 cleaved c-di-AMP into phosphoadenylyl adenosine (pApA), whereas Pde2 directly hydrolyzed c-di-AMP into AMP. Additionally, Pde2, but not Pde1, degraded pApA into AMP. Our results also demonstrated that both Pde1 and Pde2 played roles in bacterial growth, resistance to UV treatment, and virulence in a mouse pneumonia model. These results indicate that c-di-AMP homeostasis is essential for pneumococcal biology and disease.

Streptococcus pneumoniae (the pneumococcus) is part of the commensal flora of the human upper respiratory tract. It is also a major cause of an array of infections, including pneumonia, otitis media (OM), sinusitis, meningitis, and bacteremia. The pathogenesis of the bacterium is still not fully understood. Adaptation to the host niche by the pneumococcus is essential for its successful transition from a commensal to an invasive pathogen. Thus, a better understanding of how the pathogen controls its gene expression and interacts with the host is essential to more effectively control pneumococcal infections.

Several cyclic nucleotides have been shown to play important roles in bacterial gene regulation and pathogenesis. These nucleotides include cyclic AMP (cAMP), cyclic GMP (cGMP), cyclic di-GMP (c-di-GMP), cyclic di-AMP (c-di-AMP), and cyclic AMP-GMP (1, 2). Both c-di-GMP and c-di-AMP were discovered recently and were recognized as second messengers utilized by many bacteria, including bacterial pathogens during infection.

c-di-GMP regulates many biological cascades in bacteria (3, 4). It is synthesized from two GTP molecules by diguanylate cyclase through a highly conserved GGDEF domain and hydrolyzed into phosphoguanylyl adenosine (pGpG) by phosphodiesterase enzymes containing a highly conserved EAL domain. Another c-di-GMP phosphodiesterase that contains an HD-GYP domain breaks down c-di-GMP directly into two GMPs (4). c-di-GMP plays a role in the pathogenesis of many bacteria (5–14). *Vibrio cholerae vieA* encodes a c-di-GMP phosphodiesterase, and deletion of this gene led to attenuation in an infant mouse model of cholera (13, 14). This is consistent with the overexpression of a diguanylate cyclase, which resulted in the inhibition of cholera toxin production. *Salmonella enterica* serovar Typhimurium *ydiV* (or *cdgR*) encodes an EAL domain protein, which is essential for bacterial survival during exposure to oxidase (15). In *Pseudomonas aeruginosa*, the mutation of either c-di-GMP phosphodiesterase gene, *pvrR* or *rocR*, also attenuated the virulence in a mouse infection model (7). In addition, c-di-GMP regulates bacterial pathogenesis through the control of motility or biofilm formation in *P. aeruginosa*, *Yersinia pestis*, *V. cholerae*, and *S.* Typhimurium (5, 10, 16–19).

Diadenylate cyclase was first identified in *Bacillus subtilis* and *Thermotoga maritima* (20). The protein was originally named DisA for *D*NA *i*ntegrity *s*canning protein *A* and participates in a DNA damage checkpoint (21). DisA consists of a diadenylate cyclase domain, a linker domain, and a DNA-binding helix-hairpin-helix (HhH) domain and converts ATP to c-di-AMP but does not use GTP, ITP, CTP, or UTP as its substrate (20). The diadenylate cyclase domain exists across eubacteria and archaea (22, 23). Most of these bacteria possess one diadenylate cyclase; however, three diadenylate cyclases were identified in *B. subtilis* (23, 24). In *B. subtilis* and *Staphylococcus aureus*, c-di-AMP can be cleaved into phosphoadenylyl adenosine (pApA) by a phosphodiesterase, which has a PAS domain, a GGDEF domain, a DHH domain, and a DHHA1 domain. DHH and DHHA1 domains are essential for the phosphodiesterase activity (25, 26). Bacterial DNA damage in *B. subtilis* reduces the levels of c-di-AMP (27), which also serves as an essential signal molecule required for cell wall peptidoglycan architecture homeostasis of the bacterium (28). In *S. aureus*, c-di-AMP controls cell size and envelope stress, biofilm formation, drug resistance, and potassium uptake (25, 29–32). In addition, several reports indicate that c-di-AMP represents a putative bacterial secondary signaling molecule that triggers a cytosolic

Received 3 July 2013 Accepted 3 September 2013
Published ahead of print 6 September 2013
Address correspondence to Guangchun Bai, baig@mail.amc.edu.
* Present address: Yinlan Bai, Department of Microbiology, Fourth Military Medical University, Xi'an, China.
Copyright © 2013, American Society for Microbiology. All Rights Reserved.
doi:10.1128/JB.00769-13

TABLE 1 Bacterial strains and plasmids used in this study

Strain or plasmid	Description[a]	Source or reference
S. pneumoniae strains		
D39	*S. pneumoniae* serotype 2	63
ST581	D39 with *rpsL1* allele; Strep^r	42
ST2718	Δ*pde1*::Janus cassette in ST581; Kan^r	This study
ST2719	Δ*pde2*::Janus cassette in ST581; Kan^r	This study
ST2729	In-frame deletion mutant of *pde1* in ST581; Strep^r	This study
ST2730	In-frame deletion of *pde1* and Δ*pde2*::Janus cassette; Kan^r	This study
ST2733	In-frame deletion mutant of *pde2* in ST581; Strep^r	This study
ST2734	In-frame deletion mutant of *pde1*and *pde2* in ST581; Strep^r	This study
ST2847	ST581(pVA838); Strep^r Erm^r	This study
ST2848	ST2733(pST2846); Strep^r Erm^r	This study
ST2849	ST2733(pVA838); Strep^r Erm^r	This study
ST2850	ST2729(pST2846); Strep^r Erm^r	This study
ST2851	ST2729(pVA838); Strep^r Erm^r	This study
E. coli strains		
DH5α	*E. coli* strain used for cloning	Laboratory stock
BL21(DE3)	*E. coli* strain used for expression	Novagen
ST2714	*E. coli* BL21(DE3)(pST2710); Kan^r	This study
ST2715	*E. coli* BL21(DE3)(pST2711); Kan^r	This study
ST2761	*E. coli* DH5α(pST2761); Ap^r	This study
ST2762	*E. coli* DH5α(pST2762); Ap^r	This study
Plasmids		
pET28a(+)	His tag expression vector; Kan^r	Novagen
pProEXHTb	His tag expression vector; Ap^r	Invitrogen
pVA838	*E. coli-S. pneumoniae* shuttle vector; Erm^r	64
pST2710	pET28a(+) carrying *S. pneumoniae dacA* ORF; Kan^r	This study
pST2711	pET28a(+) carrying *S. pneumoniae pde2* ORF; Kan^r	This study
pST2761	pProEX HTb carrying *S. pneumoniae pde1* aa 51–657 ORF; Ap^r	This study
pST2762	pProEX HTb carrying *S. pneumoniae pde1* aa 109–657 ORF; Ap^r	This study
pST2846	pVA838 carrying *S. pneumoniae pde2* promoter and ORF; Erm^r	This study

[a] Strep^r, streptomycin resistance; Kan^r, kanamycin resistance; Erm^r, erythromycin resistance; Ap^r, ampicillin resistance.

TABLE 2 Primers used in this study

Primer[a]	Oligonucleotide sequence (5′ to 3′)[b]	Purpose[c]
Mutagenesis		
Pr1097	GAGATCTAGAACCGTTTGATTTTTAATGGATAATG	Janus cassette; For
Pr1098	GAGACTCGAGCCTTTCCTTATGCTTTTGGAC	Janus cassette; Rev
Pr2874	TGACGATAATCTTGTGACGG	*dacA* upstream; For
Pr2875	TTTTCTAGATTGATAGCTATCGTCC	*dacA* upstream; Rev
Pr2876	TTTCTCGAGTTTTAAAGAACGATTGC	*dacA* downstream; For
Pr2877	CCCTGAAATACGTGTGTCAC	*dacA* downstream; rev
Pr2880	TTTTGATCCTGATAATCACG	*pde1* upstream; For
Pr2881	TTTTCTAGATGAATGATAATGGTGTCG	*pde1* upstream; Rev
Pr2882	TTTCTCGAGTGGTGCTAATTCCTATAGC	*pde1* downstream; For
Pr2883	GTGGTTCGTGACAATAGTAC	*pde1* downstream; Rev
Pr2900	TTTCTCGAGATGATAATGGTGTCGTATTC	*pde1* unmarked mutant; Rev
Pr2901	CATTTTCCCTTGTAAGATGAGG	*pde2* upstream; For
Pr2902	TTTTCTAGACTTGTATAATGCACTCTCAG	*pde2* upstream; Rev
Pr2903	TTTCTCGAGATGTAACCTTGTCAGAAGC	*pde2* downstream; For
Pr2904	ACGCTTCGTAAGCTTGGTTG	*pde2* downstream; Rev
Pr2905	TTTCTCGAGAAGTGGATAAGACTCCAAACG	*pde2* unmarked mutant; Rev
Overexpression		
Pr2895	TTTCATATGTTGGGAAGAGCGACAGATTTC	*dacA* 89-271 aa; For
Pr2879	TTTGGATCCACAAGCAAAAAAGAGTGAGG	*dacA* 89-271 aa; Rev
Pr2884	TTTCCATGGAGATTTGCCAACAAATTTTAG	*pde2* ORF; For
Pr2885	TTTAAGCTTGTTTTTAAGCAAGTTTTTTAAC	*pde2* ORF; Rev
Pr2960	GCGGATCCAAGAAACTGAGAGTGCAT	$pde1_{51\text{-}657}$; For
Pr2961	GCCTCGAGTCATTCTTCTTTCTCCTTTTC	$pde1_{51\text{-}657}$; Rev
Pr2962	GCGGATCCACCAAGGAAGATGGTGATTTTG	$pde1_{109\text{-}657}$; For

[a] The reverse primer of $pde1_{109\text{-}657}$ was identical to $pde1_{51\text{-}657}$ Rev.
[b] The restriction site is underlined if present in an oligonucleotide.
[c] For, forward primer; Rev, reverse primer.

pathway of innate immunity (27, 33–37). Such response is mediated via STING (stimulator of interferon [IFN] genes), a transmembrane protein that functions as an essential signaling adaptor (34, 38, 39). Recent reports have revealed that DDX41, a pattern recognition receptor (PRR) with a DEAD (aspartate-glutamate-alanine-aspartate) motif, plays a critical role in cyclic dinucleotide-mediated activation of type I interferon and interferon-mediated signaling (33, 40).

The presence of c-di-AMP and a diadenylate cyclase in *Streptococcus pyogenes* has been reported (41). However, cyclic dinucleotide production and homeostasis have not been explored in *S. pneumoniae*, a Gram-positive pathogen. In the present study, we identify genes associated with c-di-AMP production and degradation in *S. pneumoniae* and show that these proteins modulate bacterial growth, UV resistance, and pathogenesis. Based on our findings, we named pneumococcal SPD_1392, SPD_2032, and SPD_1153 *dacA*, *pde1*, and *pde2* and their encoded proteins DacA, Pde1, and Pde2, respectively. This is the first identification of an enzyme (Pde2) that cleaves c-di-AMP directly into AMP.

MATERIALS AND METHODS

Bacterial strains and growth conditions. The bacterial strains used in the present study are listed in Table 1. ST581, a streptomycin-resistant D39 derivative equivalent to ST594 (42) that has a recessive *rpsL* allele, *rpsL1*, was used as the parental strain. The *rpsL1* allele confers streptomycin resistance in the absence of the wild-type (WT) *rpsL*$^+$ allele (42). Pneumococci were routinely grown in Todd-Hewitt broth containing 0.5% (wt/vol) yeast extract (THY) or on tryptic soy agar (TSA) plates containing 3% (vol/vol) sheep blood. The media were supplemented with kanamycin (200 μg/ml) or streptomycin (150 μg/ml) for selection of mutants, as specified. *Escherichia coli* DH5α was used for routine cloning, and BL21(DE3) was used for expression of recombinant proteins. The *E. coli* strains were grown in Luria-Bertani (LB) broth or LB agar plates, and all strains harboring expression plasmids were grown with kanamycin at a final concentration of 25 μg/ml.

Construction of mutants in *S. pneumoniae*. The mutants of *S. pneumoniae* were generated through homologous recombination in ST581 with a counterselectable Janus cassette, which consists of a kanamycin resistance gene and a dominant WT *rpsL*$^+$ allele (43). To construct a single mutant, the upstream and downstream sequences flanking the target gene were amplified by PCR using D39 genomic DNA as the template. The upstream fragment has an XbaI site, and the downstream fragment has an XhoI site (Table 2). These fragments were digested and ligated with the XbaI- and XhoI-digested Janus cassette. The ligation product was transformed into ST581 to select a kanamycin-resistant and streptomycin-sensitive mutant.

In-frame deletion of each gene was generated by homologous recombination from a background of the kanamycin-resistant mutant. A new reverse primer with an XhoI site (Table 2) was designed to amplify the upstream sequence and ligated directly with the XhoI-digested downstream fragment. The ligation product was transformed into the kanamycin-resistant mutant to select a streptomycin-resistant but kanamycin-sensitive mutant due to loss of the Janus cassette. The in-frame deletion mutants for *pde1* and *pde2* were designated ST2729 and ST2733, respectively.

To construct a Δ*pde1* Δ*pde2* double mutant, *pde2* was replaced with the Janus cassette in the background of ST2729 to generate ST2730. The same upstream and downstream sequences used for generating the *pde2* in-frame deletion were ligated and transformed into ST2730 to obtain a Δ*pde1* Δ*pde2* in-frame deletion mutant (ST2734).

Growth curve, morphology, and UV treatment. The *S. pneumoniae* WT (ST581) and the Δ*pde1* (ST2729), Δ*pde2* (ST2733), and Δ*pde1* Δ*pde2*

(ST2734) mutants were used to determine bacterial growth, morphology, and survival after UV treatment. To generate the growth curves, approximately 10^6 CFU of each bacterial stock was inoculated into 10 ml THY broth and grown at 37°C with 5% CO_2. The growth of each strain was measured hourly by determining the optical density of the culture at 620 nm (OD_{620}).

To determine bacterial morphology, bacteria were inoculated into 10 ml THY broth and grown to an OD_{620} of 0.3 or 0.8. Samples at each time point were smeared on slides, heat fixed, and stained using a Gram-staining kit (Sigma). Bacterial morphology was then examined using a light microscope (Olympus) at ×400 magnification.

For UV treatment, 10^6 CFU of bacteria was inoculated into 10 ml THY broth and grown to an OD_{620} of 0.4 or 0.8. Samples at each time point were taken, and 10-fold serial dilutions were performed. Two microliters of each dilution was spotted onto duplicate blood agar plates. One set of plates was treated with 1 mJ/cm^2 UV radiation using a UV cross-linker (Stratagene). The other set of plates remained untreated as controls. All the plates were then incubated at 37°C with 5% CO_2 for 18 h to enumerate the CFU. The survival rate of each strain was calculated as the number of CFU detected from the UV-treated plates as a percentage of those quantified from the untreated plates.

Protein expression and purification. Open reading frames (ORFs) of *S. pneumoniae dacA*, *pde2*, and the truncated fragments encoding amino acids (aa) 51 to 657 and 109 to 657 of Pde1 were PCR amplified using the primers listed in Table 2. *S. pneumoniae* D39 genomic DNA was used as the template. The PCR products for *dacA* and *pde2* were individually cloned into the pET28a(+) vector (Novagen) between the NcoI and HindIII sites to generate pST2710 and pST2711, respectively. These plasmids were sequence verified and maintained in *E. coli* BL21(DE3) for expression. The PCR products for $pde1_{51\text{-}657}$ and $pde1_{109\text{-}657}$ were cloned into the pProEX HTb vector (Invitrogen) between the BamHI and XhoI sites to generate pST2761 and pST2762, respectively. Both plasmids were sequence verified and maintained in *E. coli* DH5α for expression.

Expression of the proteins was induced with 0.05 mM isopropyl β-D-1-thiogalactopyranoside (IPTG) at room temperature for 4 h for DacA and Pde2 or overnight at 16°C for truncated Pde1 proteins. The recombinant proteins were purified using an Ni-nitrilotriacetic acid (NTA) resin (Qiagen) with buffers, as we previously reported (44, 45). The protein concentrations were then determined using a BCA Protein Assay Kit (Thermo Scientific). The purified protein aliquots were stored at −80°C until use.

Gel filtration. Size exclusion chromatography experiments were performed with either a HiLoad 16/60 Superdex 200-pg column (GE Healthcare) for $Pde1_{109\text{-}657}$ or a Superdex 200 10/300 GL column (GE Healthcare) for $Pde1_{51\text{-}657}$ and Pde2 and connected to a Gradiphrac Automatic Sampler (Amersham Biosciences). The columns were equilibrated and eluted at a constant flow rate of 0.5 ml/min with running buffer containing 10% (vol/vol) glycerol in phosphate-buffered saline (PBS) at pH 7.4. The molecular masses of the proteins were determined by using a Gel Filtration Standard (Bio-Rad) according to the instructions for the Gel Filtration Principles and Methods (GE Healthcare).

Cleavage of BNPP. Reaction mixtures (50 μl) consisted of 50 mM Tris-HCl at a specified pH, 10 mM NaCl, 5 μM 2-mercaptoethanol, 0.1 mM specified metal cation, and 2 mM bis-*p*-nitrophenyl phosphate (BNPP). The reaction was initiated by addition of 3 μM purified $Pde1_{109\text{-}657}$ or 70 nM purified Pde2, and the reaction mixture was incubated at room temperature for 10 min for the samples with Pde2 or for 4 h for the samples with Pde1. Relative BNPP cleavage was determined by measuring the OD_{410} using a microplate reader (Spectrum Max 340PC; Molecular Devices). The assay mixtures used for metal ion screening contained 0.1 mM $CaCl_2$, $CoCl_2$, $FeCl_2$, $Fe(NO_3)_3$, $MgCl_2$, $MnCl_2$, or $ZnSO_4$. For pH analysis, reaction mixtures consisted of 50 mM Tris-HCl at pH 6.0, 6.5, 7.0, 7.5, 8.0, 8.5, 9.0, or 9.5.

HPLC and mass spectrometry (MS). Determination of the enzymatic activities of *S. pneumoniae* DacA using high-performance liquid chromatography (HPLC) was performed as reported previously (46, 47) with minor modification. Briefly, reaction mixtures (50 μl) contained 40 mM Tris-HCl (pH 7.5), 10 mM $MgCl_2$, 100 mM NaCl, and 0.1 mM ATP. The reaction was initiated by adding 10 μM pneumococcal DacA protein, incubated for 1 h at 37°C, and then terminated by adding 1 μl of 0.5 M EDTA. Finally, 20 μl of each sample was injected and separated by reverse-phase HPLC with a C_{18} column (250 by 4.6 mm; Vydac) using a Waters 625 LC system equipped with a 996 Photodiode Array Detector and a 717 Autosampler (Waters). Samples were eluted using the same buffers and program as previously reported (48). Nucleotides were monitored at 254 nm.

The reaction mixtures (10 μl) to determine the activity of Pde1 and Pde2 contained 50 mM Tris-HCl (pH 7.5), 1 mM $MnCl_2$, and 0.5 mM the indicated nucleotide. The reaction was initiated by adding Pde1 to 10 μM and incubating for 4 h at 37°C or by adding Pde2 to 2.5 μM and incubating for 1 h at 37°C. Subsequently, each reaction was terminated by adding 1 μl of 0.5 M EDTA and diluting 1:5 with water. Finally, 20 μl of each sample was injected and separated by reverse-phase HPLC. c-di-AMP and pApA standards were purchased from Biolog. AMP was purchased from Sigma. The reaction of Pde2 was further analyzed by LC-tandem MS (MS-MS) using the same chromatography and mass spectrometry settings previously described (49) and monitoring in negative-ion mode at *m/z* 657 to 134 for c-di-AMP and *m/z* 346.18 to 78.69 for AMP. Chemically synthesized c-di-AMP and AMP ranging in concentration from 0.97 nM to 250 nM were used to generate a standard curve.

Kinetic measurement of enzymatic activities of Pde1 and Pde2. The kinetic parameters were determined by monitoring the hydrolysis of c-di-AMP by Pde1 and Pde2 and the hydrolysis of pApA by Pde2 using HPLC. The assay conditions were the same as described above, except that Pde2 was incubated with pApA for 10 min. The kinetic parameters were obtained by fitting the enzymatic activities at various substrate concentrations to a Michaelis-Menten equation using Prism 5 version 5.0a (GraphPad Software).

Preparation and detection of bacterial c-di-AMP. Bacteria were grown in 10 ml THY to an OD_{620} of 0.3 or 0.8. One milliliter of culture was harvested and resuspended in 500 μl of 50 mM Tris-HCl (pH 8.0). The suspension was sonicated for 20 s (10 s on with a 15-s interval) followed by boiling for 5 min, and the bacterial debris was removed by centrifugation for 5 min at 13,000 rpm. The supernatant was then used to detect c-di-AMP using an enzyme-linked immunosorbent assay (ELISA) that we developed at Albany Medical College (patent pending). This method was developed based on the identification of a *c*-di-AMP *b*inding *p*rotein (CabP) in *S. pneumoniae* with high affinity and specificity in interaction with c-di-AMP (Y. Bai, J. Yang, T. Zarrella, Y. Zhang, D. W. Metzger, and G. Bai, unpublished data). Briefly, a 96-well plate was coated with CabP at 10 μg/ml at 4°C for at least 14 h. The plate was then washed and blocked with 1% bovine serum albumin (BSA) for 1 h. Samples and purified c-di-AMP (Biolog) standards were mixed with 25 nM biotin-labeled c-di-AMP (Biolog) and incubated for 2 h. After thorough washing, the plate was incubated with horseradish peroxidase-conjugated streptavidin (Thermo Scientific) for 1 h. The peroxidase was finally detected with *o*-phenylenediamine dihydrochloride (OPD) (Sigma) as a substrate and measured at OD_{492}. The c-di-AMP levels in the samples were calculated based on the standard curve and were normalized by actual OD_{620} readings of each culture.

Preparation of polyclonal antibodies and Western blot analysis. Antibodies were generated similarly to our previous description (46). Briefly, five female BALB/c mice (Taconic) were immunized subcutaneously with 50 μg of either $Pde1_{51\text{-}657}$ or Pde2 emulsified 1:1 with alum (Thermo Scientific) in 100 μl and boosted twice biweekly with the same amount of protein and adjuvant. The specificity of sera was confirmed by Western blotting with purified His-$Pde1_{51\text{-}657}$ and His-Pde2, respectively.

For Western blot analysis, purified proteins or bacterial lysates were separated by sodium dodecyl sulfate-polyacrylamide gel electrophoresis (SDS-PAGE), transferred onto polyvinylidene difluoride (PVDF) mem-

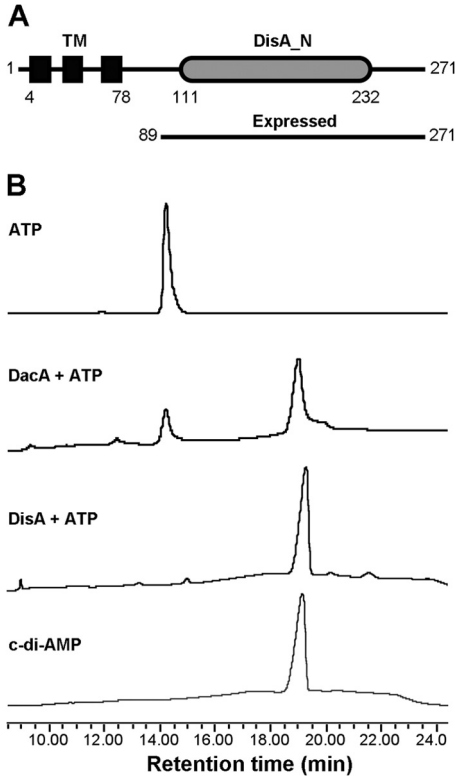

FIG 1 Domain architecture and activity of *S. pneumoniae* DacA. (A) Domain architecture of DacA. The numbers indicate the positions of amino acids in the full-length protein. TM, transmembrane domain. (B) Enzymatic activity of DacA. ATP was incubated with purified *S. pneumoniae* DacA, and the reaction mixture was separated using HPLC. ATP and c-di-AMP standards, as well as the reaction with purified *B. subtilis* DisA, were used as controls.

branes, and sequentially probed with antisera and with a peroxidase-conjugated goat anti-mouse IgG secondary antibody (Thermo Scientific). Peroxidase detection was carried out with the ECL Western blotting detection reagent and analysis system (Thermo Scientific).

Infection of mice. This study was carried out in strict accordance with the recommendations in the *Guide for the Care and Use of Laboratory Animals* of the National Research Council. The protocol was approved by the Institutional Animal Care and Use Committee of Albany Medical College. The *S. pneumoniae* WT (ST581), Δ*pde1* (ST2729), Δ*pde2* (ST2733), and Δ*pde1* Δ*pde2* (ST2734) strains were grown to an OD_{620} of 0.4 in THY broth, washed, and diluted to 10^8 CFU/ml using PBS. Six- to 8-week old female BALB/c mice (Taconic) were inoculated intranasally with 50 μl (5×10^6 CFU) of bacteria ($n = 8$ per group). The mice were subsequently monitored for 9 days.

RESULTS

***S. pneumoniae* SPD_1392 is a diadenylate cyclase.** c-di-AMP and c-di-GMP are signaling molecules that have been recognized in a number of bacteria. However, these nucleotides and their associated genes have not been explored in *S. pneumoniae*. In this study, we analyzed the genome of the *S. pneumoniae* D39 strain (50) and were unable to identify a protein with a typical diguanylate cyclase GGDEF domain in the bacterium. It is likely that either *S. pneumoniae* cannot produce c-di-GMP or the nucleotide is produced by an atypical diguanylate cyclase. In contrast, SPD_1392 encodes a protein with a DisA_N domain (50) (Fig. 1A), suggesting that this protein might have diadenylate cyclase activity, similar to DisA, DacA (also referred to as CdaA or YbbP), and DacB (also referred to as CdaS or YoiJ) of *B. subtilis*. Therefore, we designated SPD_1392 DacA, for *dia*denylate *c*yclase. The amino acid sequence of *S. pneumoniae* DacA shares 46.8% identity with the DacA proteins of *Listeria monocytogenes* (36) and *B. subtilis* (23, 24) but shares only 15.6% and 13.3% identity with the DisA proteins of *B. subtilis* (20) and *Mycobacterium tuberculosis* (previously named DacA) (46), respectively. Genetically, *S. pneumoniae dacA* is the first gene of the *dacA-cdaR-glmM* locus, similar to the *dacA* genes of *B. subtilis*, *S. aureus*, and *L. monocytogenes*. Three transmembrane helices were identified at the N terminus in *S. pneumoniae* DacA by using the TMHMM server (http://www.cbs.dtu.dk/services/TMHMM-2.0/). We were unable to express full-length DacA in *E. coli*; thus, we expressed its C-terminal domain (Fig. 1A), purified it to homogeneity, and analyzed its activity using HPLC. Our results showed that the protein converted ATP to c-di-AMP, similar to *B. subtilis* DisA (Fig. 1B), indicating that it functions as a diadenylate cyclase.

We tried five times to delete *S. pneumoniae dacA* by homologous recombination but failed to generate a Δ*dacA* mutant. This is consistent with the report that *dacA* is an essential gene in the pathogen (51).

***S. pneumoniae* SPD_2032 and SPD_1153 are c-di-AMP phosphodiesterases.** *B. subtilis* GdpP (formerly YybT) and *S. aureus* GdpP have been identified as c-di-AMP phosphodiesterases (25, 26, 53). Both proteins possess two transmembrane helices, a PAS domain, an atypical GGDEF domain, a DHH domain, and a DHHA1 domain. Experimental evidence showed that the C-terminal DHH and DHHA1 region is essential for c-di-AMP phosphodiesterase activity (25, 26). We analyzed the D39 genome and found that a protein encoded by SPD_2032 (*pde1*) has the same domain structures as GdpP (Fig. 2A). In addition, another protein encoded by SPD_1153 (*pde2*) also possesses DHH and DHHA1 domains (Fig. 2B), but not the other domains of Pde1, suggesting that this protein may also have c-di-AMP phosphodiesterase activity.

We engineered two truncated Pde1 proteins to remove either the transmembrane domain ($Pde1_{51-657}$) or both the transmembrane and PAS domains ($Pde1_{109-657}$). The proteins $Pde1_{51-657}$, $Pde1_{109-657}$, and Pde2 were then purified to homogeneity. Both the $Pde1_{51-657}$ and $Pde1_{109-657}$ proteins showed uniformly high-order oligomerization (not shown). A similar result has also been reported with *B. subtilis* GdpP (26). In contrast, Pde2 displayed a molecular mass of ~70 kDa in solution (not shown), which is consistent with Pde2 existing as a dimer.

In order to optimize the catalytic activities of these proteins, we first used BNPP, a nonspecific substrate of phosphatase and phosphodiesterase, to determine the enzymatic activities of $Pde_{109-657}$ and Pde2 under different conditions. Our results showed that both proteins preferred Mn^{2+} from the metal cations that we tested (Fig. 2C and D). In terms of pH, both $Pde1_{109-657}$ and Pde2 proteins exhibited the highest enzymatic activity at pH 8.5 (Fig. 2E and F). The preference of Pde_{51-657} was similar to that of $Pde1_{109-657}$ in all these assays (not shown).

We determined the phosphodiesterase activities of the pneumococcal Pde1 and Pde2 proteins toward cleavage of c-di-AMP. Our results showed that $Pde1_{51-657}$ cleaved c-di-AMP exclusively into pApA (Fig. 3A). This result is consistent with the activity of *B. subtilis* GdpP (26). In contrast, Pde2 hydrolyzed c-di-AMP solely into AMP (Fig. 3A), which differs from the result with Pde1. Using

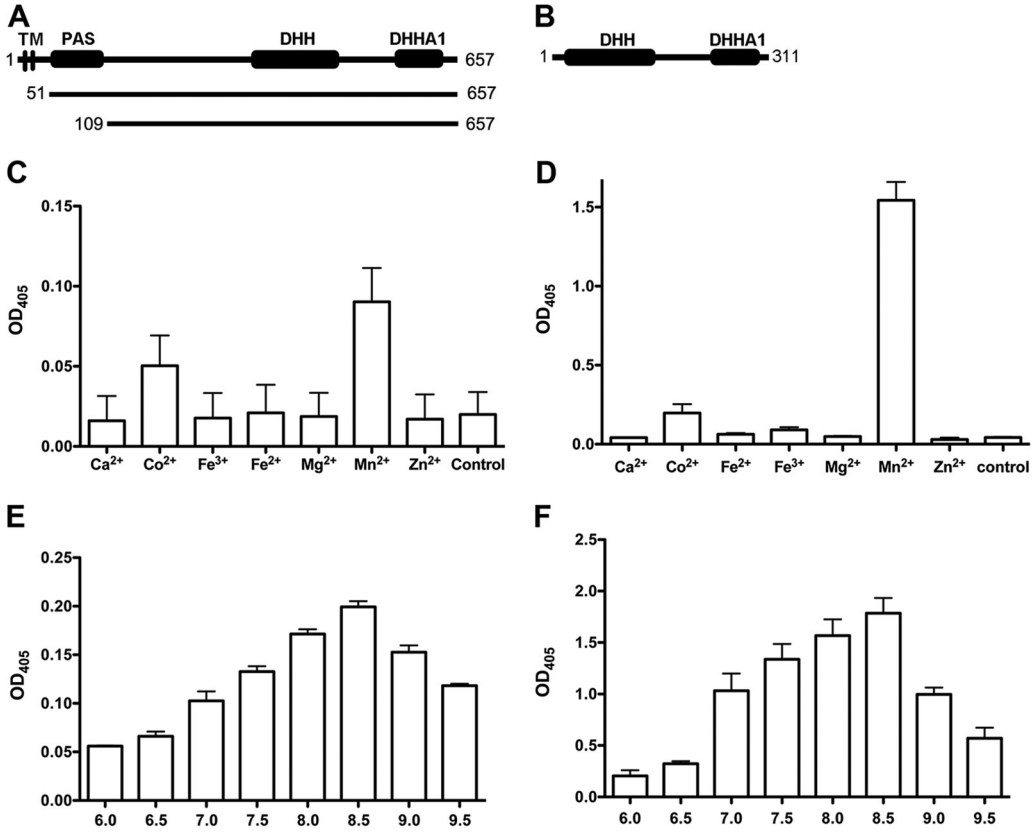

FIG 2 Cleavage of BNPP by *S. pneumoniae* Pde1 and Pde2. (A and B) Domain architectures of Pde1 (A) and Pde2 (B). Two different constructs of Pde1, $Pde1_{51\text{-}657}$ and $Pde1_{109\text{-}657}$ as indicated by the amino acid positions, were expressed and purified. (C and D) Cleavage of BNPP by $Pde1_{109\text{-}657}$ (C) and Pde2 (D) in the presence of different metal cations (no cation was present in the control reaction). (E and F) Cleavage of BNPP by $Pde1_{109\text{-}657}$ (E) and Pde2 (F) under different pH conditions. The data shown in panels C to F are the means of three independent experiments. The error bars denote the standard error of the mean (SEM).

LC–MS-MS, we confirmed that c-di-AMP was degraded to AMP by Pde2 (Fig. 3B). Additionally, Pde2 was also capable of converting pApA to AMP, whereas Pde1 showed no activity toward pApA (Fig. 3A). The activity of $Pde1_{109\text{-}657}$ was similar to that of $Pde1_{51\text{-}657}$ in all the assays (not shown), suggesting that the PAS domain does not affect the enzymatic specificity against the tested nucleotides. These results indicate that both Pde1 and Pde2 possess c-di-AMP phosphodiesterase activity, but their cleavage products are different (Fig. 3C). Our kinetics result showed that c-di-AMP was cleaved comparably by $Pde1_{51\text{-}657}$ (V_{max} = 101.6 ± 31.32 nmol mg^{-1} min^{-1}; K_m = 36.40 ± 17.43 μM) and Pde2 (V_{max} = 48.92 ± 12.71 nmol mg^{-1} min^{-1}; K_m = 16.75 ± 8.70 μM) (Fig. 4A), whereas Pde2 preferred pApA (V_{max} = 333.5 ± 61.21 μmol mg^{-1} min^{-1}; K_m = 23.96 ± 7.78 μM) (Fig. 4B) to c-di-AMP. Therefore, the cleavage product of c-di-AMP by Pde1 might be rapidly hydrolyzed into AMP by Pde2 (Fig. 3C).

Both Pde1 and Pde2 play a role in controlling bacterial c-di-AMP levels. In order to explore the biological functions of both Pde1 and Pde2 in *S. pneumoniae*, we generated mutant strains, including Δ*pde1* (ST2729), Δ*pde2* (ST2733), and Δ*pde1* Δ*pde2* (ST2734). From the genetic analysis, *pde1* is the first gene in a putative operon of 4 or 5 genes (Fig. 5A), and *pde2* may also be in an operon with SPD_1154 (Fig. 5B). Deletion of either *pde1* or *pde2* simply by replacement with a drug resistance marker may result in polar effects. Therefore, we constructed all these mutants with in-frame deletions to avoid polar effects on downstream genes (Fig. 5A and B). All three mutants were verified by PCR (not shown) and Western blot analysis using specific antibodies against Pde1 and Pde2, respectively (Fig. 5C).

The c-di-AMP levels in all three mutants were compared to those in the parental strains. Deletion of either *pde1* or *pde2* resulted in only a moderate increase of the c-di-AMP levels compared to the parental strain (Fig. 5D). However, deletion of both genes exhibited up to a 4-fold increase in c-di-AMP levels compared to that of the parental strain (Fig. 5D). This result suggests that c-di-AMP is a biological substrate of both Pde1 and Pde2 and that the two enzymes both contribute to pneumococcal c-di-AMP homeostasis.

Both Pde1 and Pde2 play a role in pneumococcal growth. It has been reported that *S. aureus* GdpP plays a role in controlling bacterial cell size and envelope stress (25). In this study, we determined the roles of Pde1 and Pde2 in pneumococcal growth. All three mutants and the parental strain were grown to early and mid-log phases and were stained to determine their morphologies. Our results showed that in early log phase, the bacterial chains of both Δ*pde1* and Δ*pde2* strains were slightly shorter than that of the WT, and the change in the Δ*pde1* Δ*pde2* double mutant was more dramatic (Fig. 6A). In mid-log phase, the lengths of the chains of all three mutants were significantly shorter than that of the WT (Fig. 6A), indicating that both Pde1 and Pde2 play a role in

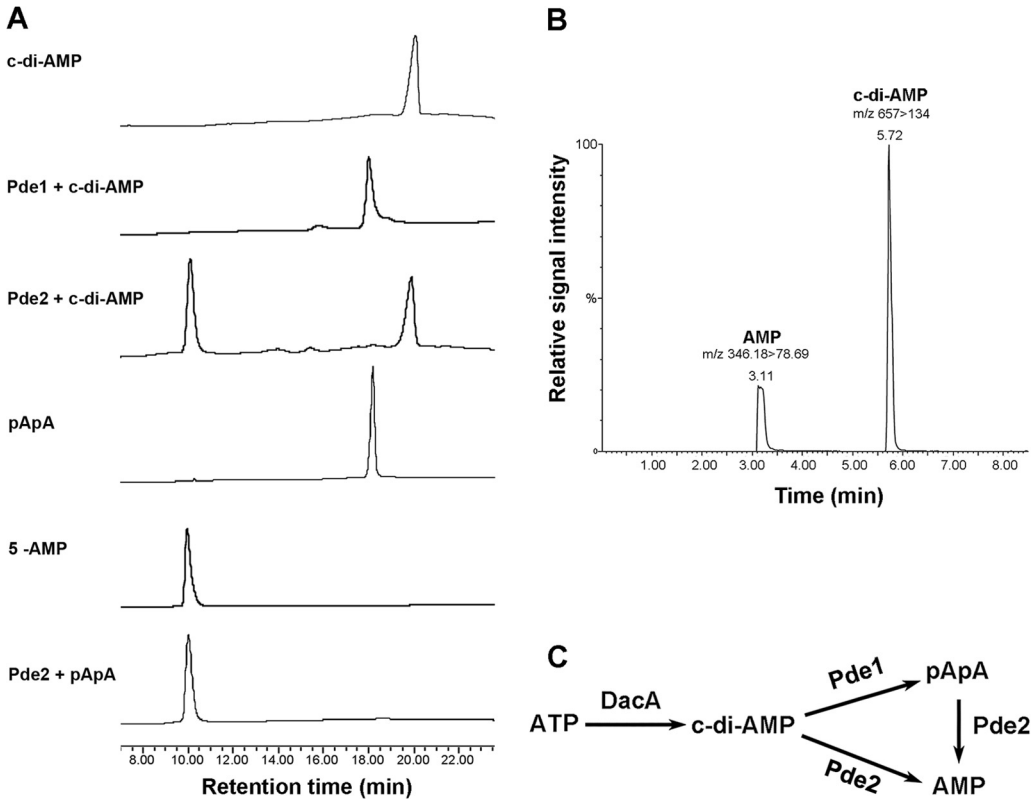

FIG 3 Phosphodiesterase activities of *S. pneumoniae* Pde1 and Pde2. (A) $Pde1_{51-657}$ or Pde2 protein was incubated with c-di-AMP or pApA, as indicated. Each sample was separated by HPLC and monitored at 254 nm. c-di-AMP, pApA, and AMP were used as standards. (B) Verification that AMP is the sole degradation product from c-di-AMP catalyzed by Pde2 using LC–MS-MS. AMP and c-di-AMP were eluted at 3.11 min and 5.72 min, respectively, which were identical to their standards (not shown). The *m/z* of each nucleotide is indicated. (C) Summary of the catalytic activities of pneumococcal DacA, Pde1, and Pde2 in homeostasis of c-di-AMP.

pneumococcal chain formation. This result is consistent with the reports that increased c-di-AMP reduces the cell size of *S. aureus* and promotes sporulation of *B. subtilis* (25, 27).

The growth curves of the WT and the three mutants were determined at OD_{620}. The results showed that both Δ*pde1* and Δ*pde2* reduced the growth rate slightly, and the double mutant synergized the reduction (Fig. 6B). This result differs from a previous report that no difference between the WT and the mutants was observed when they were grown *in vitro* (52). The difference between the two studies may have been produced by the methodology used to generate the mutants.

Pde1 orthologs in *B. subtilis* and *Lactococcus lactis* have been shown to play a role in stress response (26, 54). Additionally, it is also well established that both DisA and GdpP in *B. subtilis* are responsive to DNA damage (20, 27). In this study, we determined the pneumococcal response to UV treatment using *S. pneumoniae* WT (ST581), Δ*pde1* (ST2729), Δ*pde2* (ST2733), and Δ*pde1* Δ*pde2* (ST2734) strains. Our results showed that ~30% of the WT bacteria survived after UV radiation at 1 mJ/cm^2. However, approximately 8 to 9% of Δ*pde1* bacteria survived after the same UV treatment. The survival rates of both Δ*pde2* and Δ*pde1* Δ*pde2* bacteria were less than 0.5% (Fig. 6C). These results indicate that both Pde1 and Pde2

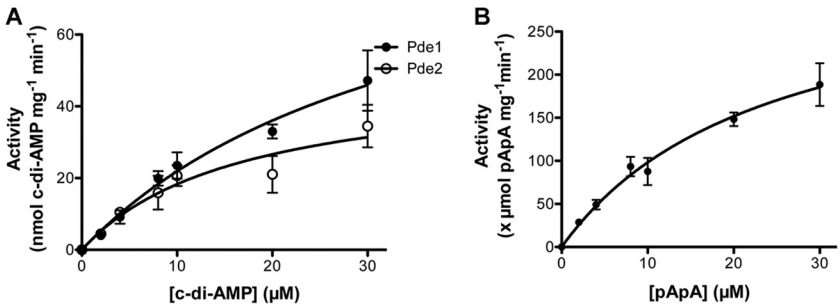

FIG 4 Cleavage of c-di-AMP and pApA by *S. pneumoniae* Pde1 and Pde2. (A) c-di-AMP at indicated concentrations was cleaved by Pde1 or Pde2 for 1 h. The enzymatic activity was determined as nmol c-di-AMP cleaved per mg protein per min. (B) pApA was cleaved by Pde2 for 10 min. Enzymatic activity was determined as μmol pApA cleaved by per mg protein per min. Note that different units are displayed for cleaved c-di-AMP (A) and pApA (B). The error bars indicate the SEM.

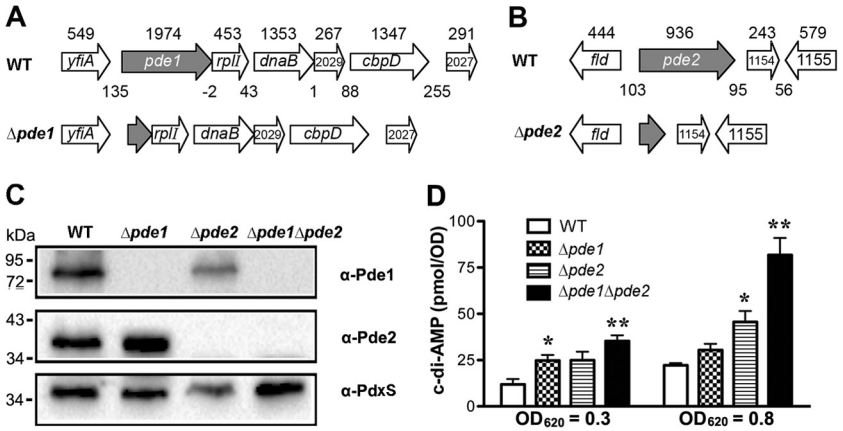

FIG 5 Construction of in-frame deletion mutants of *pde1* and *pde2* in *S. pneumoniae*. (A and B) The in-frame deletion mutants of *S. pneumoniae pde1* (A) and *pde2* (B) were generated using homologous recombination. The size (in bp) of each ORF is indicated above the gene. The length (in bp) of each intergenic region is also marked between adjacent genes. (C) Western blot analysis to verify the deletion of *pde1* and *pde2* using antibodies against Pde1 and Pde2, respectively. Subsequent blotting with a mouse anti-PdxS antibody (62) served as a loading control. (D) Detection of bacterial c-di-AMP levels. Bacteria were grown in THY broth to an OD_{620} of 0.3 or 0.8. Each sample was then harvested, resuspended in 50 mM Tris-HCl (pH 8.0), and sonicated. The bacterial debris was removed, and the supernatant was taken to detect c-di-AMP levels using ELISA. The concentration of each sample was normalized with the actual OD_{620}. The data shown are the means of three independent experiments. The error bars denote the SEM. *, $P < 0.05$; **, $P < 0.01$ in a two-tailed *t* test using Prism 5.0a (GraphPad Software).

play a role in response to UV radiation, and Pde2 contributes more to response against UV damage than Pde1.

Both Pde1 and Pde2 are essential in pneumococcal pathogenesis. The roles of Pde1 and Pde2 in pneumococcal pathogenesis have been well characterized, including adherence to human epithelial cells, as well as colonizing and causing OM, pneumonia, and bacteremia in various mouse infection models (52). In the mouse pneumonia competitive-infection model, bacterial loads

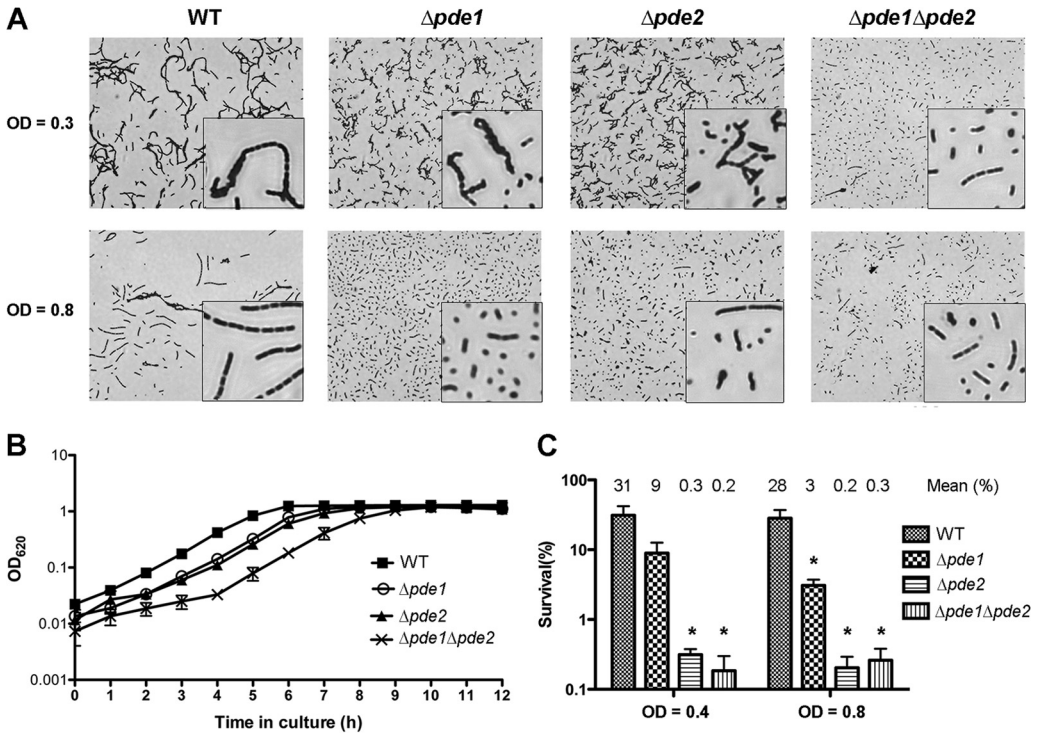

FIG 6 Growth phenotypes of the *S. pneumoniae* Δ*pde1* and Δ*pde2* mutants. (A) Morphology of the WT, Δ*pde1*, Δ*pde2*, and Δ*pde1* Δ*pde2* strains after Gram staining. The images were taken at a magnification of ×400. The insets are enlarged an additional 4-fold. The results shown are representative of three independent experiments. (B) Growth curves of the WT, Δ*pde1*, Δ*pde2*, and Δ*pde1* Δ*pde2* strains in THY broth. The same CFU from the bacterial stocks were inoculated, and bacterial growth was monitored hourly. The data shown are the means of three independent experiments. The error bars denote the SEM. (C) Response of WT, Δ*pde1*, Δ*pde2*, and Δ*pde1* Δ*pde2* strains to UV treatment. Bacterial serial dilutions were spotted onto TSA plates either with or without treatment with UV radiation. The plates were then incubated overnight, and the CFU were enumerated to determine the survival percentage of each bacterial strain. The data shown are the means of three independent experiments. The error bars denote the SEM. *, $P < 0.05$ in a two-tailed *t* test using Prism 5.0a (GraphPad Software).

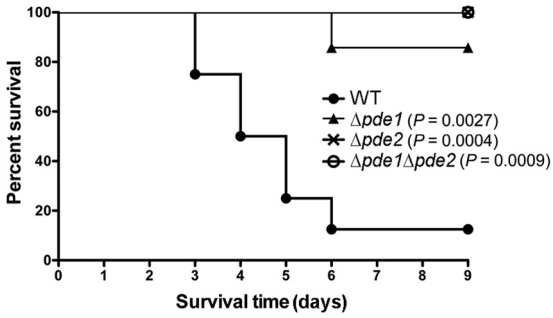

FIG 7 Infection of mice with the pneumococcal phosphodiesterase mutants. Approximately 5×10^6 CFU of the WT, Δ*pde1*, Δ*pde2*, or Δ*pde1* Δ*pde2* strain was inoculated intranasally in 50 μl PBS, and the mice were subsequently monitored for 9 days. The indicated *P* values are the statistical results for each mutant compared to the WT and analyzed by the log-rank (Mantel-Cox) test using Prism 5.0a (GraphPad Software).

in both the lung homogenate and the bronchoalveolar lavage fluid (BALF) of mice were numerated 48 h postinfection. Both Pde1 and Pde2 are essential for virulence (52).

In this study, we also determined the roles of Pde1 and Pde2 in pneumococcal virulence using a mouse pneumonia model. We compared the survival rates of mice infected with the WT, Δ*pde1*, Δ*pde2*, or Δ*pde1* Δ*pde2* strain. Our results showed that the median survival time of the WT-infected mice was 4.5 days, while the mice infected with the mutant strains, with the exception of one mouse infected with Δ*pde1*, all survived until the end time point (Fig. 7). This result indicates that the virulence of all the three mutants was significantly attenuated compared to the parental strain, which is consistent with the observation of the bacterial loads (52). Therefore, both Pde1 and Pde2 are required during pneumococcal infection.

DISCUSSION

In this study, *S. pneumoniae dacA* was identified as an ortholog of *B. subtilis dacA* (24). In *B. subtilis*, three diadenylate cyclases have been reported, DisA, DacA, and DacB (23, 24). Analysis using the TMHMM server revealed that the DacA proteins of *B. subtilis*, *S. pneumoniae*, *L. monocytogenes*, and *S. aureus* all possess three transmembrane helices, whereas *B. subtilis* DisA and DacB, as well as *M. tuberculosis* DisA, are cytoplasmic. Recent studies showed that *disA*, *dacA*, or *dacB* alone could be disrupted in *B. subtilis*, but a triple mutant of these genes could not be generated in the bacterium unless one of these cyclases was provided (24, 28). These observations clearly indicate that c-di-AMP, rather than any one particular diadenylate cyclase, is required for the viability of *B. subtilis* (24). Interestingly, *dacA* is an essential gene in *S. pneumoniae* (51), similar to those in *L. monocytogenes* and *S. aureus* (25, 36). Moreover, *dacA* encodes the only diadenylate cyclase identified in the three bacterial species. Therefore, the essentiality of *dacA* in these bacteria is very likely due to the need for c-di-AMP for bacterial viability.

It is interesting that the presence of c-di-AMP or c-di-GMP is relatively distinct between Gram-positive and Gram-negative bacteria (23). The majority of diguanylate cyclases have been identified in Gram-negative bacteria, whereas diadenylate cyclases have been reported mostly in Gram-positive bacteria. The presence of c-di-GMP signaling in Gram-positive bacteria has been directly demonstrated only in *B. subtilis* (55, 56) and the spore-forming, obligate anaerobe *Clostridium difficile* (57). We were unable to find any GGDEF motif in *S. pneumoniae* proteins. The Pde1 ortholog in *Streptococcus mutans*, AAN59731, has been implicated as a diguanylate cyclase and plays a role in biofilm formation (58). However, a typical GGDEF motif is absent in the protein, and its ortholog in *B. subtilis* is unable to generate c-di-GMP from GTP (26). Moreover, we showed that pneumococcal Pde1 functions as a phosphodiesterase, similar to its ortholog in *B. subtilis* (26). Therefore, there is no evidence that c-di-GMP is present in *Streptococcus* spp.

In a previous study, an ortholog of *S. pneumoniae* Pde2 in *S. mutans* was characterized as 3′-phosphoadenosine-5′-phosphate (pAp) phosphatase, which dephosphorylates pAp to AMP (59). Additionally, both Pde1 and Pde2 have been reported to contribute to pneumococcal virulence and to confer protection against pneumococcal disease (52). In this study, we explored whether these pneumococcal proteins were able to hydrolyze c-di-AMP and other nucleotides. Both of the DHH domain proteins in *S. pneumoniae* were shown to function as c-di-AMP phosphodiesterases. However, the cleavage products of Pde1 and Pde2 differ. Pde1 orthologs and similar enzymatic activities have been demonstrated in *B. subtilis*, *S. aureus*, and *L. monocytogenes* (25–27, 54, 60). However, cleavage of c-di-AMP by Pde2 has not been reported, but its orthologs can be found in all these bacteria, indicating that the bacteria all likely have more than one enzyme that cleaves c-di-AMP. Pde2 is an ortholog of *B. subtilis* YtqI (also named NrnA), which has been shown to degrade nanoRNA (RNA oligonucleotides of ≤5 nucleotides) and dephosphorylates pAp to AMP (61). In addition, the Pde2 ortholog in *S. mutans* degrades pAp (59), while *B. subtilis* GdpP is unable to hydrolyze pAp (26). Thus, the activities of these enzymes differ substantially in substrate preferences and catalytic products. Interestingly, in the c-di-GMP networks, when high initial levels of c-di-GMP were provided as the substrate, pGpG was detected as an intermediate degradation product by the HD_GYP domain protein. In contrast, we could not detect pApA in reactions with c-di-AMP and Pde2.

All the reported Pde1-like proteins have two transmembrane helices. In contrast, the Pde2-like proteins in these bacteria are all cytoplasmic, based on analysis using the TMHMM server (http://www.cbs.dtu.dk/services/TMHMM-2.0/). The presence of more than one c-di-AMP phosphodiesterase in a bacterium raises the following possibilities: (i) the two enzymes are responsible for local c-di-AMP pools within the bacterium due to their different distributions; (ii) their hydrolyzed products, pApA and AMP, have different biological roles; and (iii) these proteins may have other biological functions, in addition to cleaving c-di-AMP.

S. pneumoniae c-di-AMP homeostasis needs to be well maintained, since pneumococcal *dacA* is an essential gene and deletion of either *pde1* or *pde2* in the pathogen resulted in defective bacterial growth. Our observations are consistent with the report that both lack and high-level accumulation of c-di-AMP in *B. subtilis* are detrimental to bacterial growth (24). Surprisingly, deletion of *pde1* and *pde2* showed similar defects in bacterial growth but different levels of resistance to UV treatment, as the Δ*pde2* strain is more sensitive to UV than the Δ*pde1* strain. These observations further support the possibility that c-di-AMP microenvironments are generated by these phosphodiesterases.

Both Pde1 and Pde2 have been shown to be essential in different pneumococcal infection models, suggesting that c-di-AMP

plays an important role during infections. It is likely that elevated bacterial c-di-AMP reduces the virulence of the pathogen. Nonetheless, it is important to understand what effector proteins and signal transduction pathways are involved in this response. Understanding the molecular basis of c-di-AMP signaling pathways will possibly provide new insights into controlling infections caused by *S. pneumoniae*.

ACKNOWLEDGMENTS

We are grateful for the technical assistance from Hongmin Li's laboratory and the Biochemistry Core at the Wadsworth Center, New York State Department of Health. We thank Gregor Witte for providing the DisA expression plasmid.

This work was supported by National Institutes of Health grant DC006917 (to D.W.M.).

REFERENCES

1. **Davies BW, Bogard RW, Young TS, Mekalanos JJ.** 2012. Coordinated regulation of accessory genetic elements produces cyclic di-nucleotides for *V. cholerae* virulence. Cell **149:**358–370.
2. **Gomelsky M.** 2011. cAMP, c-di-GMP, c-di-AMP and now cGMP: bacteria use them all! Mol. Microbiol. **79:**562–565.
3. **Camilli A, Bassler BL.** 2006. Bacterial small-molecule signaling pathways. Science **311:**1113–1116.
4. **Hengge R.** 2009. Principles of c-di-GMP signalling in bacteria. Nat. Rev. Microbiol. **7:**263–273.
5. **Hammer BK, Bassler BL.** 2009. Distinct sensory pathways in *Vibrio cholerae* El Tor and classical biotypes modulate cyclic dimeric GMP levels to control biofilm formation. J. Bacteriol. **191:**169–177.
6. **Kazmierczak BI, Lebron MB, Murray TS.** 2006. Analysis of FimX, a phosphodiesterase that governs twitching motility in *Pseudomonas aeruginosa*. Mol. Microbiol. **60:**1026–1043.
7. **Kulasakara H, Lee V, Brencic A, Liberati N, Urbach J, Miyata S, Lee DG, Neely AN, Hyodo M, Hayakawa Y, Ausubel FM, Lory S.** 2006. Analysis of *Pseudomonas aeruginosa* diguanylate cyclases and phosphodiesterases reveals a role for bis-(3′-5′)-cyclic-GMP in virulence. Proc. Natl. Acad. Sci. U. S. A. **103:**2839–2844.
8. **Lamprokostopoulou A, Monteiro C, Rhen M, Romling U.** 2010. Cyclic di-GMP signalling controls virulence properties of *Salmonella enterica* serovar Typhimurium at the mucosal lining. Environ. Microbiol. **12:**40–53.
9. **Lim B, Beyhan S, Yildiz FH.** 2007. Regulation of *Vibrio* polysaccharide synthesis and virulence factor production by CdgC, a GGDEF-EAL domain protein, in *Vibrio cholerae*. J. Bacteriol. **189:**717–729.
10. **Martinez-Wilson HF, Tamayo R, Tischler AD, Lazinski DW, Camilli A.** 2008. The *Vibrio cholerae* hybrid sensor kinase VieS contributes to motility and biofilm regulation by altering the cyclic diguanylate level. J. Bacteriol. **190:**6439–6447.
11. **Ryan RP, Lucey J, O'Donovan K, McCarthy Y, Yang L, Tolker-Nielsen T, Dow JM.** 2009. HD-GYP domain proteins regulate biofilm formation and virulence in *Pseudomonas aeruginosa*. Environ. Microbiol. **11:**1126–1136.
12. **Tamayo R, Schild S, Pratt JT, Camilli A.** 2008. Role of cyclic di-GMP during El Tor biotype *Vibrio cholerae* infection: characterization of the in vivo-induced cyclic di-GMP phosphodiesterase CdpA. Infect. Immun. **76:**1617–1627.
13. **Tischler AD, Camilli A.** 2004. Cyclic diguanylate (c-di-GMP) regulates *Vibrio cholerae* biofilm formation. Mol. Microbiol. **53:**857–869.
14. **Tischler AD, Camilli A.** 2005. Cyclic diguanylate regulates *Vibrio cholerae* virulence gene expression. Infect. Immun. **73:**5873–5882.
15. **Hisert KB, MacCoss M, Shiloh MU, Darwin KH, Singh S, Jones RA, Ehrt S, Zhang Z, Gaffney BL, Gandotra S, Holden DW, Murray D, Nathan C.** 2005. A glutamate-alanine-leucine (EAL) domain protein of Salmonella controls bacterial survival in mice, antioxidant defence and killing of macrophages: role of cyclic diGMP. Mol. Microbiol. **56:**1234–1245.
16. **Bobrov AG, Kirillina O, Perry RD.** 2007. Regulation of biofilm formation in *Yersinia pestis*. Adv. Exp. Med. Biol. **603:**201–210.
17. **Borlee BR, Goldman AD, Murakami K, Samudrala R, Wozniak DJ, Parsek MR.** 2010. *Pseudomonas aeruginosa* uses a cyclic-di-GMP-regulated adhesin to reinforce the biofilm extracellular matrix. Mol. Microbiol. **75:**827–842.
18. **Grantcharova N, Peters V, Monteiro C, Zakikhany K, Romling U.** 2010. Bistable expression of CsgD in biofilm development of *Salmonella enterica* serovar Typhimurium. J. Bacteriol. **192:**456–466.
19. **Krasteva PV, Fong JC, Shikuma NJ, Beyhan S, Navarro MV, Yildiz FH, Sondermann H.** 2010. *Vibrio cholerae* VpsT regulates matrix production and motility by directly sensing cyclic di-GMP. Science **327:**866–868.
20. **Witte G, Hartung S, Buttner K, Hopfner KP.** 2008. Structural biochemistry of a bacterial checkpoint protein reveals diadenylate cyclase activity regulated by DNA recombination intermediates. Mol. Cell **30:**167–178.
21. **Bejerano-Sagie M, Oppenheimer-Shaanan Y, Berlatzky I, Rouvinski A, Meyerovich M, Ben-Yehuda S.** 2006. A checkpoint protein that scans the chromosome for damage at the start of sporulation in *Bacillus subtilis*. Cell **125:**679–690.
22. **Corrigan RM, Grundling A.** 2013. Cyclic di-AMP: another second messenger enters the fray. Nat. Rev. Microbiol. **11:**513–524.
23. **Romling U.** 2008. Great times for small molecules: c-di-AMP, a second messenger candidate in Bacteria and Archaea. Sci. Signal. **1:**pe39. doi:10.1126/scisignal.133pe39.
24. **Mehne FM, Gunka K, Eilers H, Herzberg C, Kaever V, Stulke J.** 2013. Cyclic di-AMP homeostasis in *Bacillus subtilis*: both lack and high-level accumulation of the nucleotide are detrimental for cell growth. J. Biol. Chem. **288:**2004–2017.
25. **Corrigan RM, Abbott JC, Burhenne H, Kaever V, Grundling A.** 2011. c-di-AMP is a new second messenger in *Staphylococcus aureus* with a role in controlling cell size and envelope stress. PLoS Pathog. **7:**e1002217. doi:10.1371/journal.ppat.1002217.
26. **Rao F, See RY, Zhang D, Toh DC, Ji Q, Liang ZX.** 2010. YybT is a signaling protein that contains a cyclic dinucleotide phosphodiesterase domain and a GGDEF domain with ATPase activity. J. Biol. Chem. **285:**473–482.
27. **Oppenheimer-Shaanan Y, Wexselblatt E, Katzhendler J, Yavin E, Ben-Yehuda S.** 2011. c-di-AMP reports DNA integrity during sporulation in *Bacillus subtilis*. EMBO Rep. **12:**594–601.
28. **Luo Y, Helmann JD.** 2012. Analysis of the role of *Bacillus subtilis* sigma(M) in beta-lactam resistance reveals an essential role for c-di-AMP in peptidoglycan homeostasis. Mol. Microbiol. **83:**623–639.
29. **Banerjee R, Gretes M, Harlem C, Basuino L, Chambers HF.** 2010. A *mecA*-negative strain of methicillin-resistant *Staphylococcus aureus* with high-level beta-lactam resistance contains mutations in three genes. Antimicrob. Agents Chemother. **54:**4900–4902.
30. **Corrigan RM, Campeotto I, Jeganathan T, Roelofs KG, Lee VT, Grundling A.** 2013. Systematic identification of conserved bacterial c-di-AMP receptor proteins. Proc. Natl. Acad. Sci. U. S. A. **110:**9084–9089.
31. **Griffiths JM, O'Neill AJ.** 2012. Loss of function of the GdpP protein leads to joint beta-lactam/glycopeptide tolerance in *Staphylococcus aureus*. Antimicrob. Agents Chemother. **56:**579–581.
32. **Holland LM, O'Donnell ST, Ryjenkov DA, Gomelsky L, Slater SR, Fey PD, Gomelsky M, O'Gara JP.** 2008. A staphylococcal GGDEF domain protein regulates biofilm formation independently of cyclic dimeric GMP. J. Bacteriol. **190:**5178–5189.
33. **Parvatiyar K, Zhang Z, Teles RM, Ouyang S, Jiang Y, Iyer SS, Zaver SA, Schenk M, Zeng S, Zhong W, Liu ZJ, Modlin RL, Liu YJ, Cheng G.** 2012. The helicase DDX41 recognizes the bacterial secondary messengers cyclic di-GMP and cyclic di-AMP to activate a type I interferon immune response. Nat. Immunol. **13:**1155–1161.
34. **Sauer JD, Sotelo-Troha K, von Moltke J, Monroe KM, Rae CS, Brubaker SW, Hyodo M, Hayakawa Y, Woodward JJ, Portnoy DA, Vance RE.** 2011. The N-ethyl-N-nitrosourea-induced Goldenticket mouse mutant reveals an essential function of Sting in the in vivo interferon response to *Listeria monocytogenes* and cyclic dinucleotides. Infect. Immun. **79:**688–694.
35. **Schwartz KT, Carleton JD, Quillin SJ, Rollins SD, Portnoy DA, Leber JH.** 2012. Hyperinduction of host beta interferon by a *Listeria monocytogenes* strain naturally overexpressing the multidrug efflux pump MdrT. Infect. Immun. **80:**1537–1545.
36. **Woodward JJ, Iavarone AT, Portnoy DA.** 2010. c-di-AMP secreted by intracellular *Listeria monocytogenes* activates a host type I interferon response. Science **328:**1703–1705.
37. **Yamamoto T, Hara H, Tsuchiya K, Sakai S, Fang R, Matsuura M, Nomura T, Sato F, Mitsuyama M, Kawamura I.** 2012. *Listeria monocytogenes* strain-specific impairment of the TetR regulator underlies the

drastic increase in cyclic di-AMP secretion and beta interferon-inducing ability. Infect. Immun. **80:**2323–2332.
38. **Burdette DL, Monroe KM, Sotelo-Troha K, Iwig JS, Eckert B, Hyodo M, Hayakawa Y, Vance RE.** 2011. STING is a direct innate immune sensor of cyclic di-GMP. Nature **478:**515–518.
39. **Jin L, Hill KK, Filak H, Mogan J, Knowles H, Zhang B, Perraud AL, Cambier JC, Lenz LL.** 2011. MPYS is required for IFN response factor 3 activation and type I IFN production in the response of cultured phagocytes to bacterial second messengers cyclic-di-AMP and cyclic-di-GMP. J. Immunol. **187:**2595–2601.
40. **Bowie AG.** 2012. Innate sensing of bacterial cyclic dinucleotides: more than just STING. Nat. Immunol. **13:**1137–1139.
41. **Kamegaya T, Kuroda K, Hayakawa Y.** 2011. Identification of a *Streptococcus pyogenes* SF370 gene involved in production of c-di-AMP. Nagoya J. Med. Sci. **73:**49–57.
42. **Lu L, Ma Y, Zhang J-R.** 2006. *Streptococcus pneumoniae* recruits complement factor H through the amino terminus of CbpA. J. Biol. Chem. **281:**15464–15474.
43. **Sung CK, Li H, Claverys JP, Morrison DA.** 2001. An *rpsL* cassette, janus, for gene replacement through negative selection in *Streptococcus pneumoniae*. Appl. Environ. Microbiol. **67:**5190–5196.
44. **Bai G, Gazdik MA, Schaak DD, McDonough KA.** 2007. The *Mycobacterium bovis* BCG cyclic AMP receptor-like protein is a functional DNA binding protein in vitro and in vivo, but its activity differs from that of its *M. tuberculosis* ortholog, Rv3676. Infect. Immun. **75:**5509–5517.
45. **Bai G, McCue LA, McDonough KA.** 2005. Characterization of *Mycobacterium tuberculosis* Rv3676 (CRP_{Mt}), a cyclic AMP receptor protein-like DNA binding protein. J. Bacteriol. **187:**7795–7804.
46. **Bai Y, Yang J, Zhou X, Ding X, Eisele LE, Bai G.** 2012. *Mycobacterium tuberculosis* Rv3586 (DacA) is a diadenylate cyclase that converts ATP or ADP into c-di-AMP. PLoS One **7:**e35206. doi:10.1371/journal.pone.0035206.
47. **Christen M, Christen B, Folcher M, Schauerte A, Jenal U.** 2005. Identification and characterization of a cyclic di-GMP-specific phosphodiesterase and its allosteric control by GTP. J. Biol. Chem. **280:**30829–30837.
48. **Ryjenkov DA, Tarutina M, Moskvin OV, Gomelsky M.** 2005. Cyclic diguanylate is a ubiquitous signaling molecule in bacteria: insights into biochemistry of the GGDEF protein domain. J. Bacteriol. **187:**1792–1798.
49. **Massie JP, Reynolds EL, Koestler BJ, Cong JP, Agostoni M, Waters CM.** 2012. Quantification of high-specificity cyclic diguanylate signaling. Proc. Natl. Acad. Sci. U. S. A. **109:**12746–12751.
50. **Lanie JA, Ng WL, Kazmierczak KM, Andrzejewski TM, Davidsen TM, Wayne KJ, Tettelin H, Glass JI, Winkler ME.** 2007. Genome sequence of Avery's virulent serotype 2 strain D39 of *Streptococcus pneumoniae* and comparison with that of unencapsulated laboratory strain R6. J. Bacteriol. **189:**38–51.
51. **Song JH, Ko KS, Lee JY, Baek JY, Oh WS, Yoon HS, Jeong JY, Chun J.** 2005. Identification of essential genes in *Streptococcus pneumoniae* by allelic replacement mutagenesis. Mol. Cells **19:**365–374.
52. **Cron LE, Stol K, Burghout P, van Selm S, Simonetti ER, Bootsma HJ, Hermans PW.** 2011. Two DHH subfamily 1 proteins contribute to pneumococcal virulence and confer protection against pneumococcal disease. Infect. Immun. **79:**3697–3710.
53. **Rao F, Ji Q, Soehano I, Liang ZX.** 2011. Unusual heme-binding PAS domain from YybT family proteins. J. Bacteriol. **193:**1543–1551.
54. **Smith WM, Pham TH, Lei L, Dou J, Soomro AH, Beatson SA, Dykes GA, Turner MS.** 2012. Heat resistance and salt hypersensitivity in *Lactococcus lactis* due to spontaneous mutation of llmg_1816 (gdpP) induced by high-temperature growth. Appl. Environ. Microbiol. **78:**7753–7759.
55. **Chen Y, Chai Y, Guo JH, Losick R.** 2012. Evidence for cyclic di-GMP-mediated signaling in *Bacillus subtilis*. J. Bacteriol. **194:**5080–5090.
56. **Gao X, Mukherjee S, Matthews PM, Hammad LA, Kearns DB, Dann CE, III.** 26 July 2013. Functional characterization of core components of the *Bacillus subtilis* c-di-GMP signaling pathway. J. Bacteriol. doi:10.1128/JB.00373-13.
57. **Purcell EB, McKee RW, McBride SM, Waters CM, Tamayo R.** 2012. Cyclic diguanylate inversely regulates motility and aggregation in *Clostridium difficile*. J. Bacteriol. **194:**3307–3316.
58. **Yan W, Qu T, Zhao H, Su L, Yu Q, Gao J, Wu B.** 2010. The effect of c-di-GMP (3′-5′-cyclic diguanylic acid) on the biofilm formation and adherence of *Streptococcus mutans*. Microbiol. Res. **165:**87–96.
59. **Zhang J, Biswas I.** 2009. 3′-Phosphoadenosine-5′-phosphate phosphatase activity is required for superoxide stress tolerance in *Streptococcus mutans*. J. Bacteriol. **191:**4330–4340.
60. **Pozzi C, Waters EM, Rudkin JK, Schaeffer CR, Lohan AJ, Tong P, Loftus BJ, Pier GB, Fey PD, Massey RC, O'Gara JP.** 2012. Methicillin resistance alters the biofilm phenotype and attenuates virulence in *Staphylococcus aureus* device-associated infections. PLoS Pathog. **8:**e1002626. doi:10.1371/journal.ppat.1002626.
61. **Mechold U, Fang G, Ngo S, Ogryzko V, Danchin A.** 2007. YtqI from *Bacillus subtilis* has both oligoribonuclease and pAp-phosphatase activity. Nucleic Acids Res. **35:**4552–4561.
62. **El Qaidi S, Yang J, Zhang JR, Metzger DW, Bai G.** 2013. The vitamin B_6 biosynthesis pathway in *Streptococcus pneumoniae* is controlled by pyridoxal 5′-phosphate and the transcription factor PdxR and has an impact on ear infection. J. Bacteriol. **195:**2187–2196.
63. **Avery OT, Macleod CM, McCarty M.** 1944. Studies on the chemical nature of the substance inducing transformation of pneumococcal types: induction of transformation by a desoxyribonucleic acid fraction isolated from pneumococcus type III. J. Exp. Med. **79:**137–158.
64. **Macrina FL, Evans RP, Tobian JA, Hartley DL, Clewell DB, Jones KR.** 1983. Novel shuttle plasmid vehicles for Escherichia-Streptococcus transgeneric cloning. Gene **25:**145–150.